



Figures and figure supplements

VEGFR-2 conformational switch in response to ligand binding

Sarvenaz Sarabipour et al

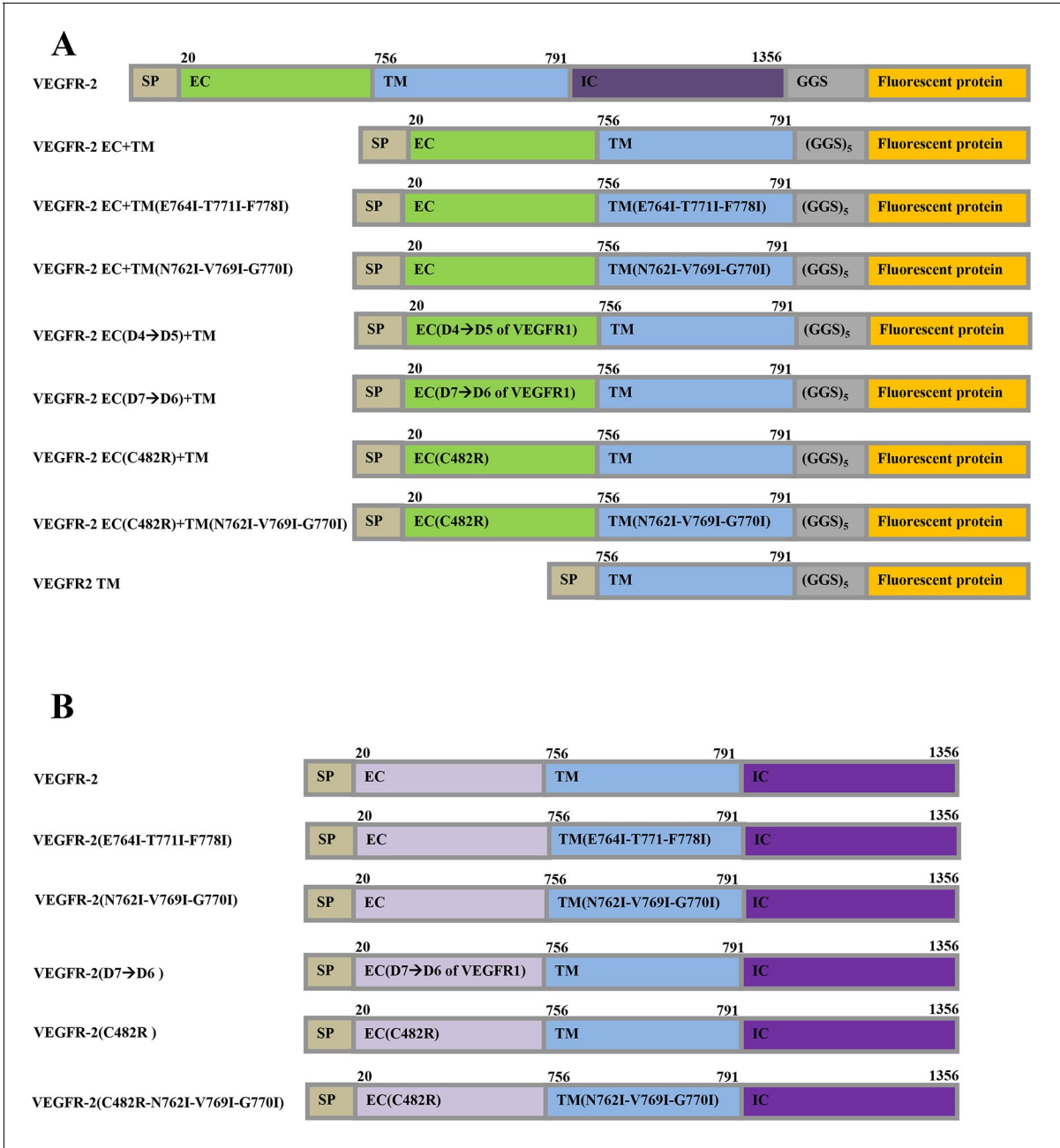


Figure 1. The plasmid constructs used in this study. **(A)** The constructs used in the FRET experiments. The full-length receptors had fluorescent proteins attached to their C-termini via a flexible GGS linker. The truncated receptors had the intracellular domain substituted with a fluorescent protein, which was attached to the TM domain via a longer flexible (GGS)₅ linker. SP: signal peptide, EC: extracellular domain, TM: transmembrane domain, IC: Intracellular domain of VEGFR-2. Fluorescent protein was either YFP or mCherry. Amino acid residue numbers are shown above the constructs. **(B)** The constructs used in the Western blotting experiments.
DOI: [10.7554/eLife.13876.003](https://doi.org/10.7554/eLife.13876.003)

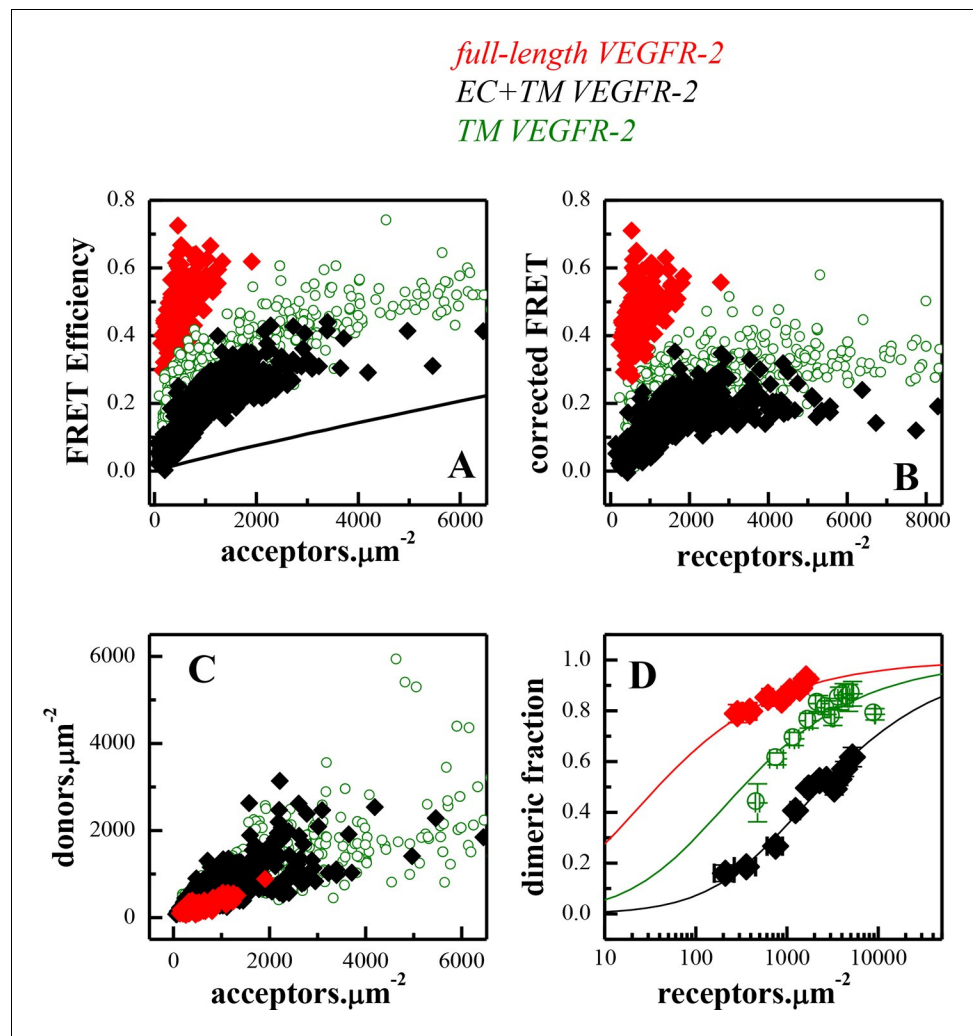


Figure 2. FRET measurements of VEGFR-2 dimerization in CHO plasma membranes. (A) FRET efficiencies as a function of acceptor concentration for full length VEGFR-2 (solid red diamonds), EC+TM VEGFR-2 (solid black diamonds), and TM VEGFR-2 (open olive circles). Two hundred to 500 individual vesicles were imaged in at least three independent experiments. Each data point here corresponds to a single vesicle. The solid line is the so-called 'stochastic' or 'proximity' FRET which arises when donors and acceptors approach each other within distances of 100 Å or so, in the absence of specific interactions (King et al., 2014). (B) FRET efficiencies corrected for stochastic FRET (King et al., 2014). (C) Donor concentration versus acceptor concentration in individual vesicles, for the three VEGFR-2 constructs. (D) Dimeric fractions versus total receptor concentrations, for the full-length VEGFR-2 (solid red diamonds), EC+TM VEGFR-2 (solid black diamonds), and the TM domains only (open olive circles). The measured dimeric fractions are binned and are shown with the symbols, along with the standard errors. The solid lines are the best fits of a monomer-dimer equilibrium model to the single-vesicle FRET data. Full-length VEGFR-2 has a significant propensity for dimerization in the absence of ligand. The contribution of the intracellular (IC) domain to dimerization is favorable, while the contribution of extracellular (EC) domain is inhibitory (see Table 1).

DOI: 10.7554/eLife.13876.004

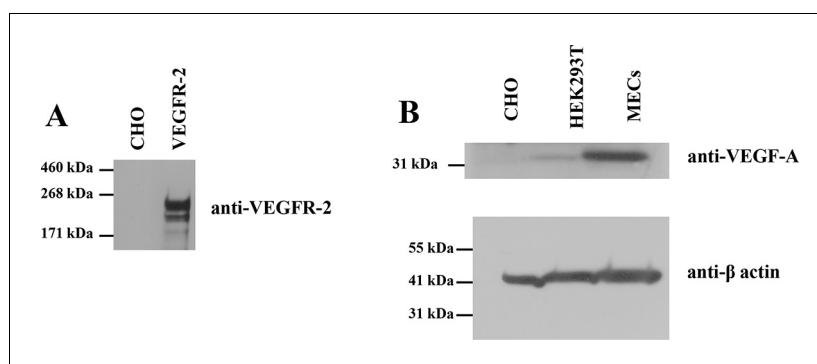


Figure 2—figure supplement 1. (A) CHO cells do not express VEGFR-2 endogenously. (B) CHO cells do not express VEGF endogenously. Here, CHO cells, HEK293T cells, and MECs (microvascular endothelial) cells were stained for VEGF-A. Lysates were reduced before loading.

DOI: [10.7554/eLife.13876.005](https://doi.org/10.7554/eLife.13876.005)

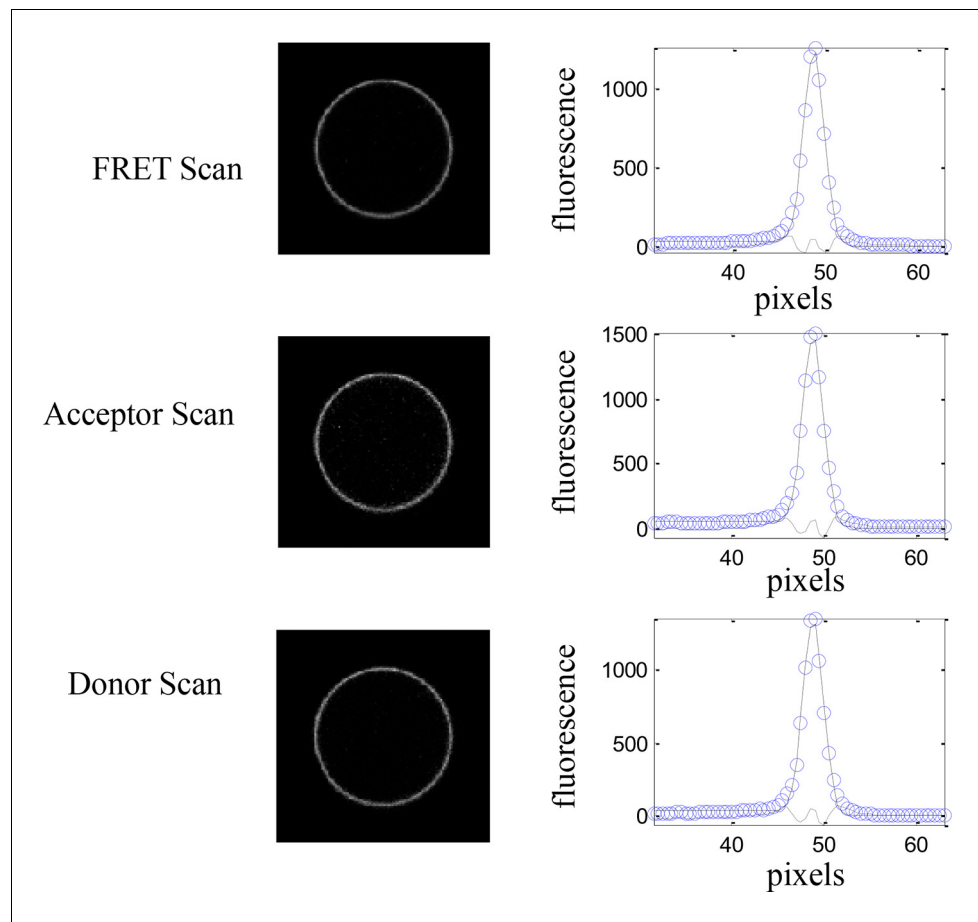


Figure 2—figure supplement 2. A single vesicle imaged and analyzed in the FRET, acceptor, and donor channels. Images were acquired with a Nikon laser scanning confocal microscope. The intensity across the membrane (open blue symbols) is fit to a Gaussian (solid line) after background correction. Shown also is the residual from the fit ([Chen et al., 2010](#)).

DOI: [10.7554/eLife.13876.006](https://doi.org/10.7554/eLife.13876.006)

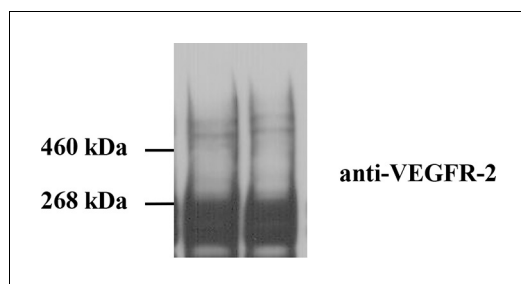


Figure 2—figure supplement 3. Cross-linking of CHO cells expressing full-length wild-type VEGFR-2. Cells were starved for 24 hr to ensure that there was no ligand present. Staining with anti-VEGFR-2 antibodies shows the presence of a glycosylated monomer band at MW ~240 kDa and glycosylated dimer band at MW ~480 kDa. These results support the FRET results that VEGFR-2 forms ligand-independent dimers in the plasma membrane.

DOI: [10.7554/eLife.13876.007](https://doi.org/10.7554/eLife.13876.007)

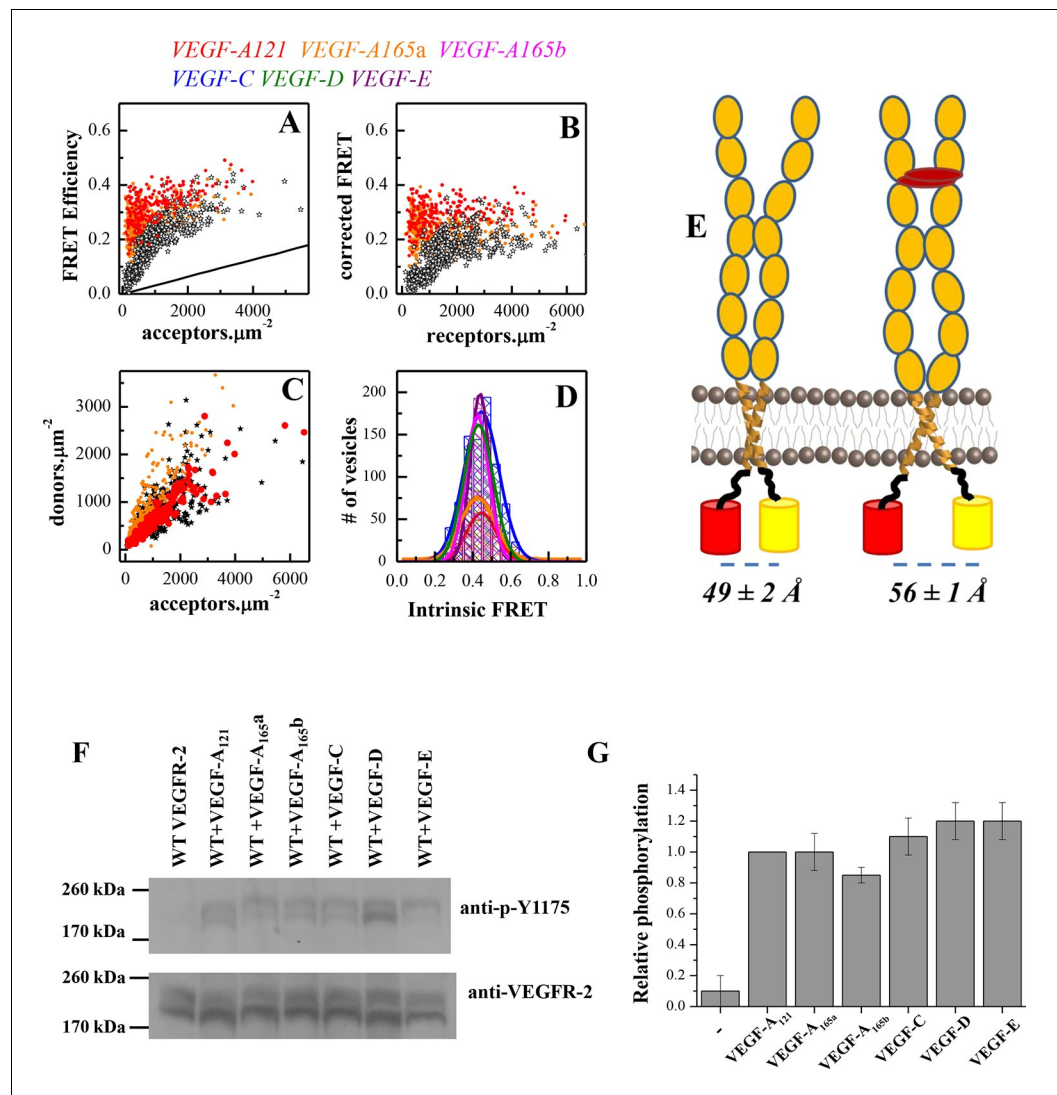


Figure 3. A conformational change in the TM domain dimer upon ligand binding increases VEGFR-2 phosphorylation. (A) FRET efficiency measured as a function of acceptor concentration for EC+TM VEGFR-2, in the absence of ligand and in the presence of $3 \mu\text{g} \cdot \text{ml}^{-1}$ VEGF-A₁₂₁ and VEGF-A_{165a}. Two hundred to 500 individual vesicles were imaged in at least three independent experiments. Each data point corresponds to a single vesicle. The stochastic FRET contribution (King et al., 2014) is shown as a solid line. Black stars: FRET data without ligand. (B) FRET efficiencies for individual vesicles, corrected for the stochastic FRET contribution. There is no dependence on receptor concentration, indicative of constitutive dimerization. (C) Donor concentrations versus acceptor concentrations. (D) Intrinsic FRET values, measured for VEGFR-2 EC+TM in the presence of $3 \mu\text{g} \cdot \text{ml}^{-1}$ of VEGF-A₁₂₁, VEGF-A_{165a}, VEGF-A_{165b}, VEGF-C, VEGF-E, and VEGF-D. (E) Graphical representation of the ligand-induced changes in distance between fluorescent proteins, and the inferred changes in TM domain structures. (F) The six VEGF ligands increase VEGFR-2 phosphorylation, to the same extent. A representative Western Blot comparing the phosphorylation of Tyr 1175 in the absence of ligand, and in the presence of six VEGF ligands, at concentrations of $3 \mu\text{g} \cdot \text{ml}^{-1}$. Only the top bands, corresponding to mature fully glycosylated receptors, are considered here. Phosphorylation is significantly increased upon ligand addition, with the increase being as high as 10 times. (G) Quantification of Western blot results for the fully glycosylated receptors (top bands), in the presence of the six ligands. VEGFR-2 phosphorylation in the presence of the six ligands is very similar.

DOI: 10.7554/eLife.13876.009

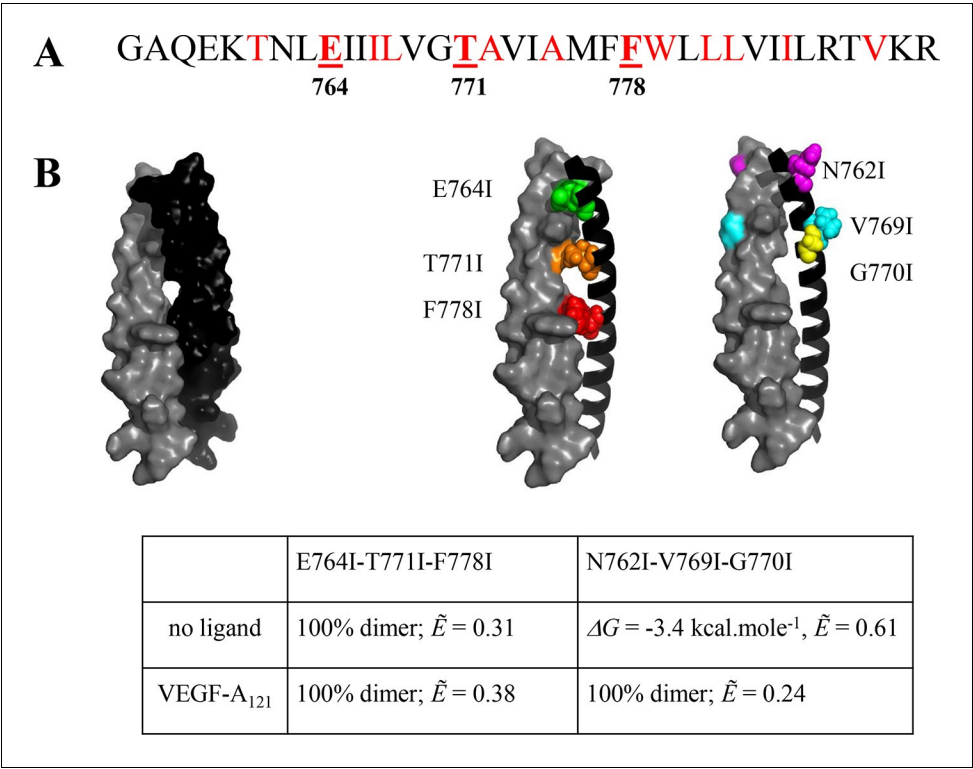


Figure 4. The published NMR structure of the isolated VEGFR-2 TM domain (Manni et al., 2014b) is consistent with the unliganded TM dimer structure observed in the FRET experiments. (A) Amino acid sequence of wild-type VEGFR-2 TM domain. The amino acids that mediate helix-helix contacts in the NMR dimer structure (Manni et al., 2014b) are shown in red. (B) The NMR structure, with two sets of amino acids highlighted. Left: a space-fill model of the wild-type VEGFR-2 TM dimer, based on NMR experiments. Center: E764, T771, and F778 help mediate helix-helix contacts in the NMR structure (Manni et al., 2014b) (also shown bold and underlined in (A)). Right: N762, V769, and G770 face away from the dimer interface, into the membrane. Two sets of mutations: a E764I-T771I-F778I set and a N762I-V769I-G770I set, were engineered. Table: Results of FRET experiments for the two sets of mutants (see also Table 1). The dimerization of the unliganded EC+TM construct was affected by the E764I-T771I-F778I but not by the N762I-V769I-G770I set of mutations, suggesting that the unliganded VEGFR-2 TM dimer is stabilized by contacts involving E764, T771, and/or F778, as in the NMR structure. At least one of the amino acids N762, V769, and G770 forms direct intermolecular contacts in the TM domain in the ligand-bound state.

DOI: 10.7554/eLife.13876.010

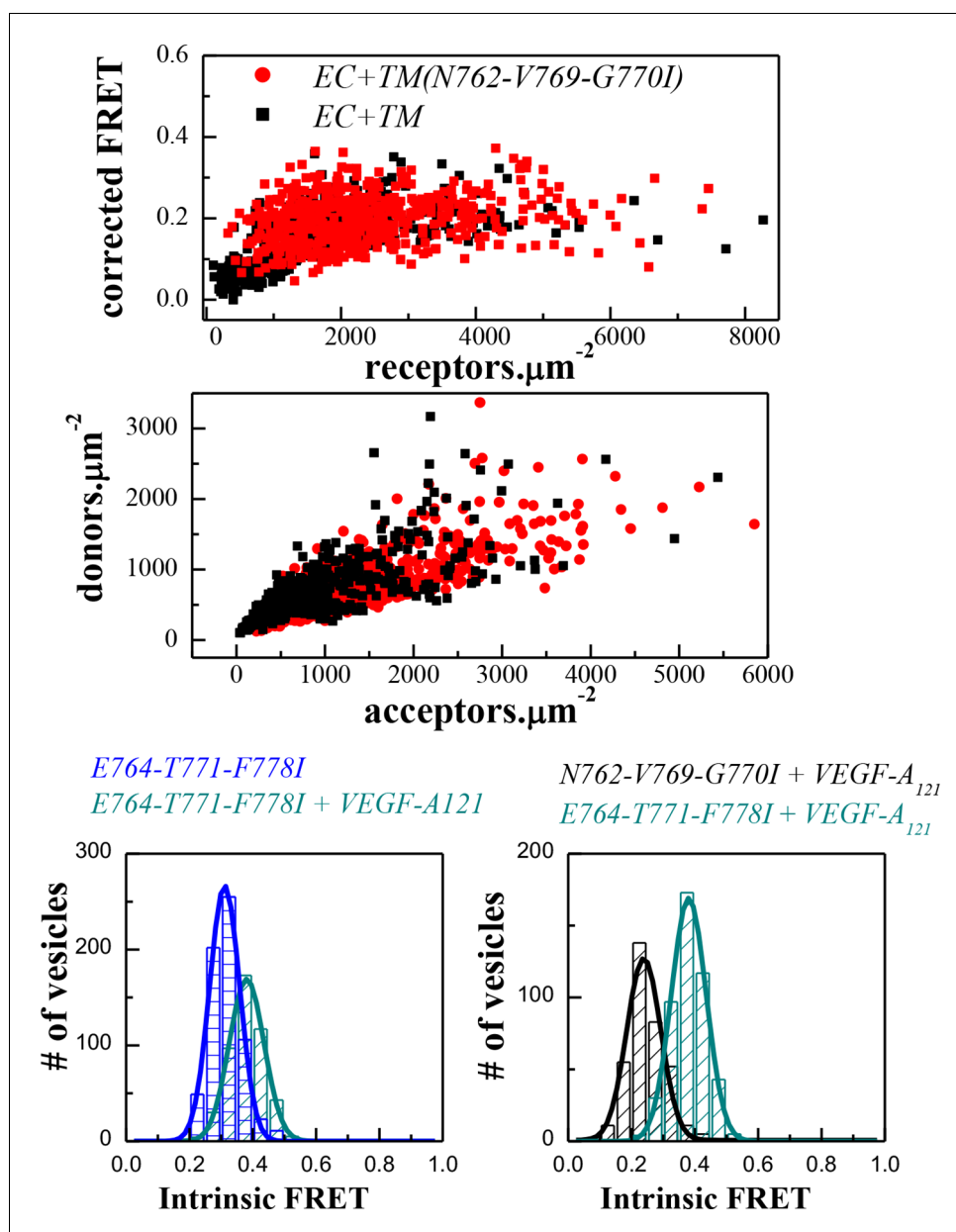


Figure 4—figure supplement 1. FRET data, reporting on the effects of the E764I-T771I-F778I and N762I-V769I-G770I sets of mutations, engineered in the EC+TM VEGFR-2 plasmids.

DOI: [10.7554/eLife.13876.011](https://doi.org/10.7554/eLife.13876.011)

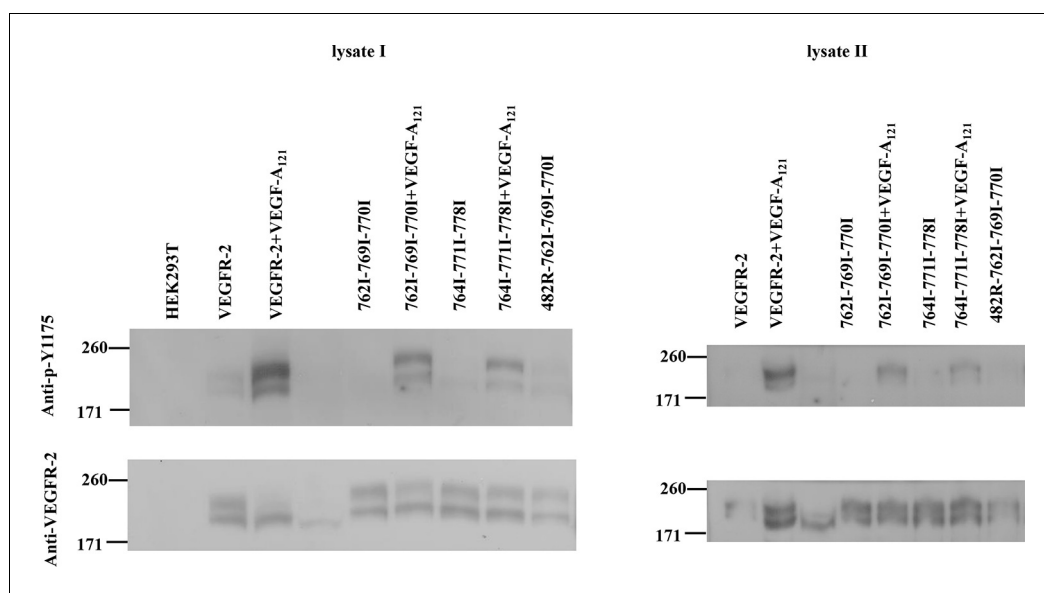


Figure 4—figure supplement 2. All mutations in the TM domain decrease VEGFR-2 phosphorylation.

DOI: [10.7554/eLife.13876.012](https://doi.org/10.7554/eLife.13876.012)

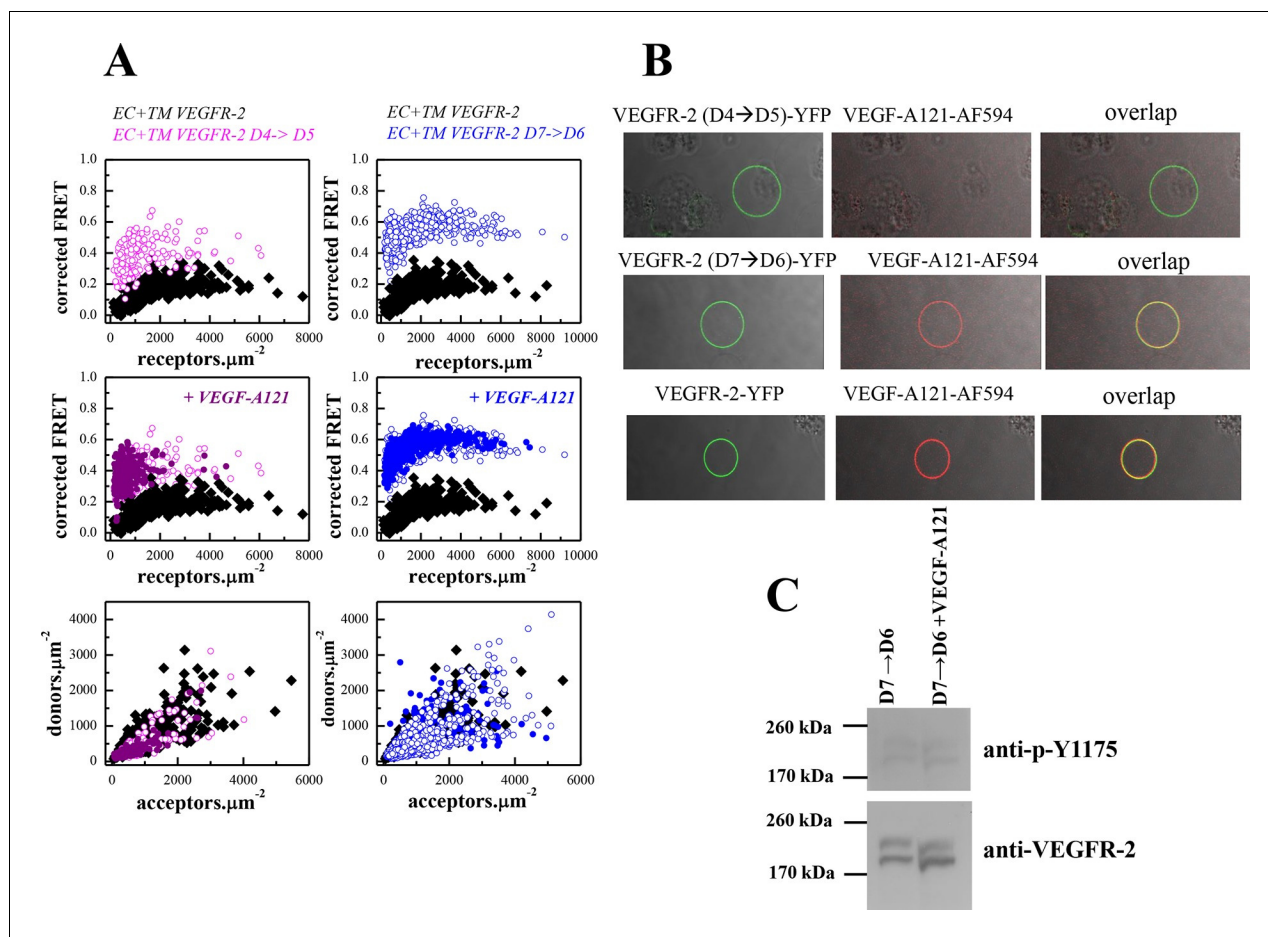


Figure 5. The D4 and D7 mutants do not respond to ligand. **(A)** FRET measurements for the D4 and D7 mutants, in the absence of ligand and in the presence of VEGF-A₁₂₁. The two mutants exhibit much higher FRET efficiencies, compared to the wild-type. The ligand, at $3 \mu\text{g} \cdot \text{ml}^{-1}$, has no effect on receptor dimerization. **(B)** VEGF-A₁₂₁ does not bind to the D4→D5 mutant, when it binds to the wild-type and the D7→D6 mutant. Here, a single vesicle containing YFP-tagged mutant receptors (two top rows) or wild-type receptors (bottom row) is shown after incubation with $3 \mu\text{g} \cdot \text{ml}^{-1}$ AlexaFluor 594-labeled VEGF-A (VEGF-A₁₂₁-AF594) (SibTech Inc., CT). Note the differences in the middle column, showing the fluorescence of the bound ligand. **(C)** Western blots comparing the phosphorylation of the full-length D7→D6 mutant in the absence and presence of VEGF-A₁₂₁. The top band corresponds to the mature fully glycosylated form of VEGFR-2. The ligand does not increase the phosphorylation.

DOI: [10.7554/eLife.13876.013](https://doi.org/10.7554/eLife.13876.013)

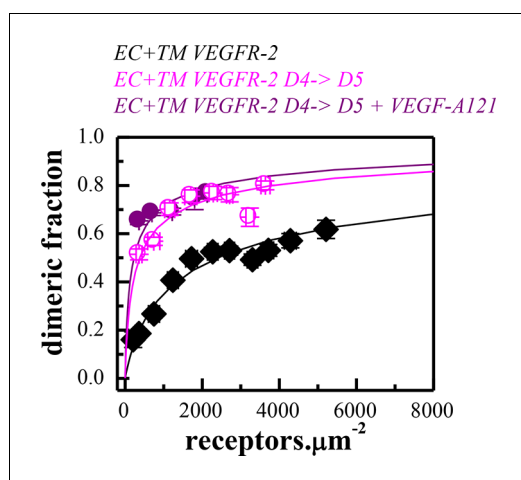


Figure 5—figure supplement 1. Dimerization curves for the wild-type VEGFR-2 in the absence of ligand, the D4→D5 mutant in the absence of ligand, and the D4→D5 mutant in the presence of VEGF-A₁₂₁.

DOI: [10.7554/eLife.13876.014](https://doi.org/10.7554/eLife.13876.014)

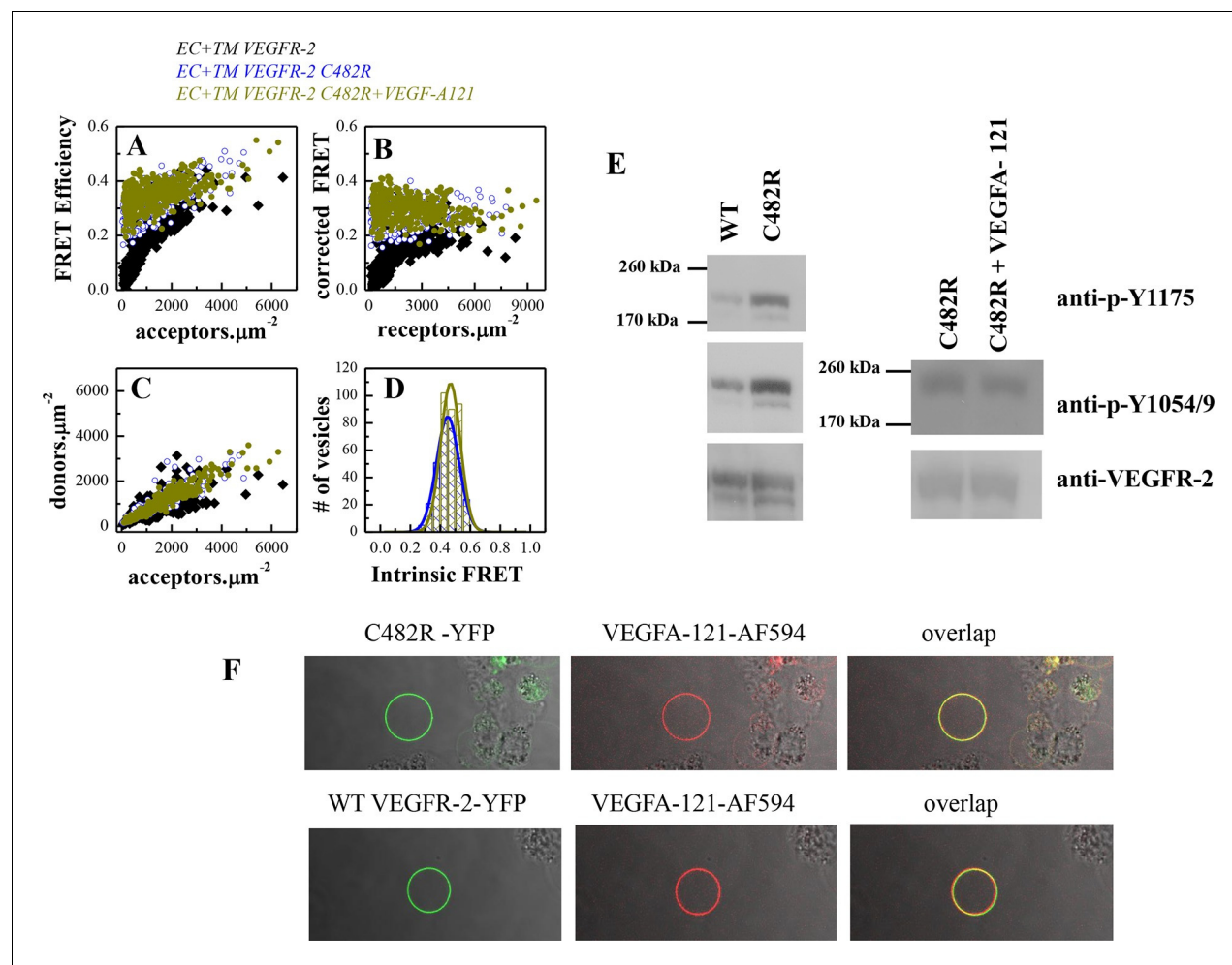


Figure 6. The C482R mutation mimics the effect of bound ligand by promoting a structural change in the EC+TM VEGFR-2 dimer. (A) FRET efficiencies determined in individual plasma-membrane-derived vesicles. (B) Corrected FRET as a function of receptor concentration. The corrected FRET for the mutant does not depend on receptor concentration, demonstrating that the mutant is a constitutive dimer in the presence and absence of ligand. (C) Measured donor versus acceptor concentrations in each vesicle. (D) Histograms of measured FRET efficiencies for the mutant, yielding Intrinsic FRET values of ~0.42. (E) Western blots showing an increase in phosphorylation due to the C482R mutation, in the absence of ligand, and no further increase upon ligand treatment. The top bands correspond to the mature fully glycosylated form of VEGFR-2. (F) Confocal images of VEGF-A₁₂₁-AF594 binding to EC+TM VEGFR-2 C482R in CHO membrane vesicles, demonstrating that the C482R mutant is capable of ligand binding.

DOI: [10.7554/eLife.13876.015](https://doi.org/10.7554/eLife.13876.015)

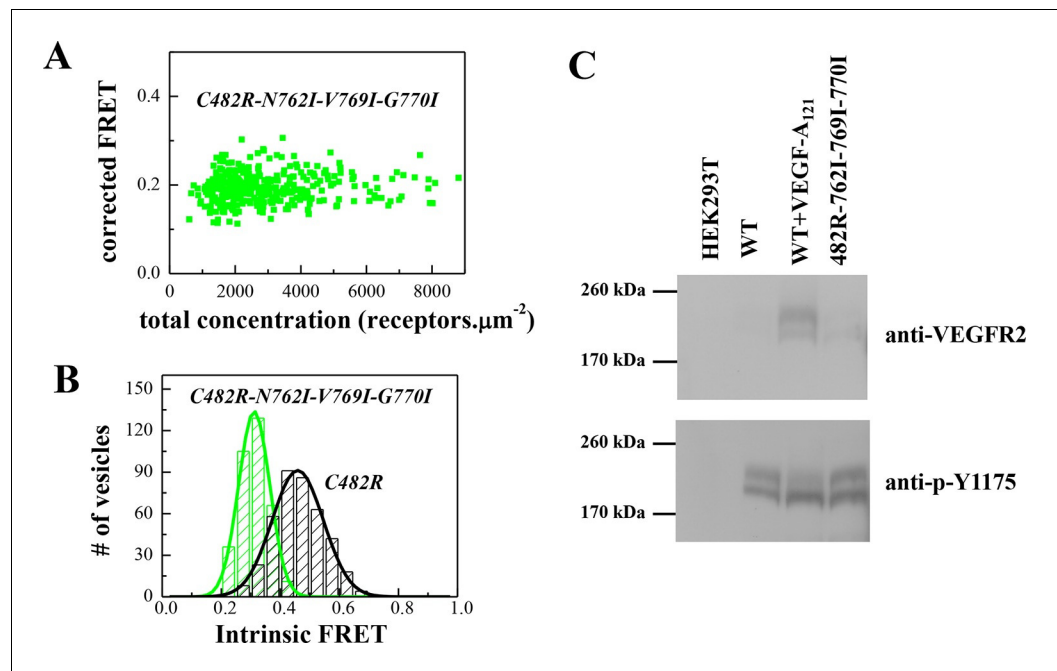


Figure 7. The N762I-V769I-G770I set of mutations in the TM domain of the C482R mutant receptor alters dimer structure and activity, as in the case of the ligand-bound wild-type (see **Figure 4**). (A) Corrected FRET efficiencies for the EC+TM C482R-N762I-V769I-G770I mutant as a function of receptor concentration, indicative of constitutive dimers. (B) Histograms of Intrinsic FRET measured for the EC+TM C482R mutant and the EC+TM C482R-N762I-V769I-G770I mutant. The TM domain mutations alter Intrinsic FRET and thus the structure of the C482R dimer. (C) The N762I-V769I-G770I set of mutations obliterate the activity of the C482R mutant, as in the case of the ligand-bound wild type.

DOI: [10.7554/eLife.13876.016](https://doi.org/10.7554/eLife.13876.016)

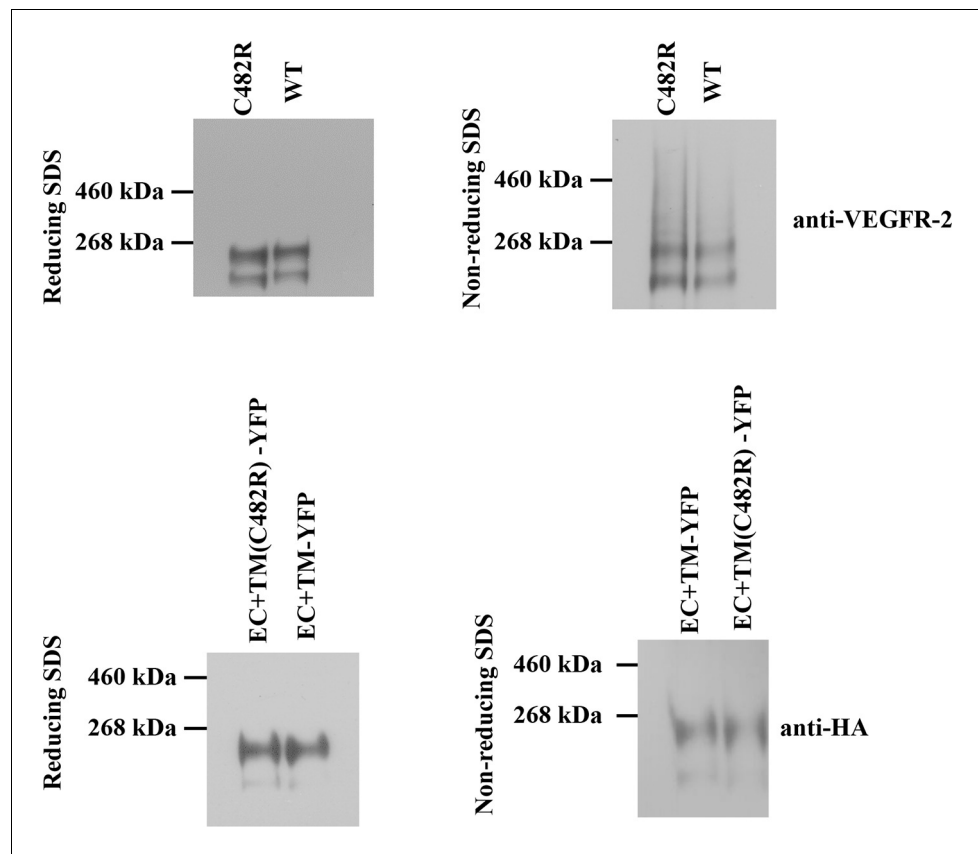


Figure 7—figure supplement 1. Left: Western blots under reducing conditions, for full length C482R VEGFR-2 and for the C482R EC+TM-YFP VEGFR-2 construct. Right: Western blots under non-reducing conditions. No dimeric bands were observed under any conditions. The constitutive dimerization of the C482R mutant is not due to cysteine-induced intermolecular cross-linking mediated by unpaired cysteines.

DOI: [10.7554/eLife.13876.017](https://doi.org/10.7554/eLife.13876.017)

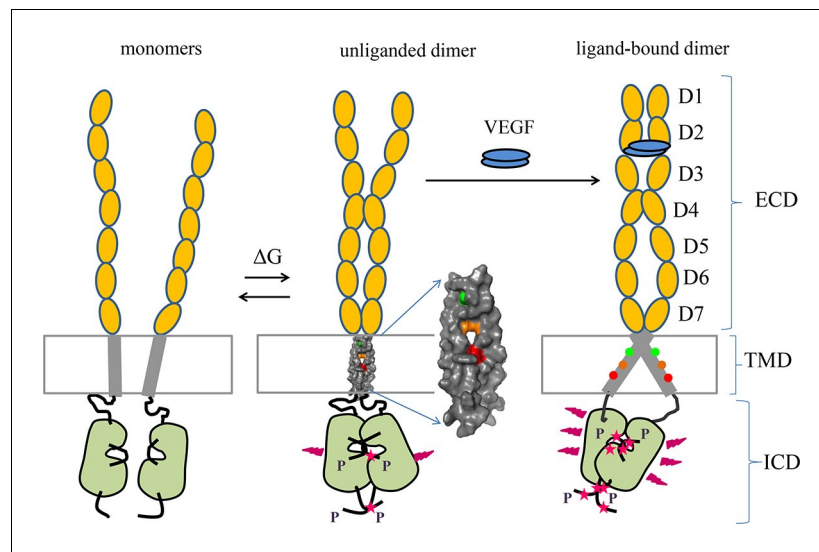


Figure 8. Proposed model for VEGFR-2 activation. VEGFR-2 pre-dimerizes in the absence of ligand. Under physiological conditions, corresponding to 10 to 100 VEGFR-2 molecules per square micron, 30 to 60% of the receptors are dimeric. The dimers are stabilized by homotypic contacts in D4-7 in the EC domain, TM interactions that involve amino acids E764, T771, and/or F778, and contacts between the intracellular domains. The EC domain, as a whole, inhibits dimerization. The ligand-free dimers are phosphorylated, to a low degree. (B) Ligand binding induces a rotation in the TM helices and the formation of a different TM dimer configuration, such that amino acids E764, T771, and F778 now face the lipid membrane, away from the TM dimer interface. These structural changes increase the separation between the C-termini of the TM helices, promoting an increase in receptor phosphorylation and activation. Contacts between D4 and D7 persist in the ligand-bound state.

DOI: [10.7554/eLife.13876.018](https://doi.org/10.7554/eLife.13876.018)